Identification and Analysis of Ancient Ship Wood Excavated at Nantong Hydraulic Site

Qinghui Gao,[a,*] Jiang You,[b] Xiaomei Liao,[b] and Zhigao Wang [a,*]

The Nantong Ancient Ship refers to an ancient Chinese wooden ship of the late Ming Dynasty excavated in Nantong city in December 2022. This paper identifies the wood and discusses its related analysis. Wood samples extracted from the Nantong Ancient Ship were studied from the viewpoints of anatomy, physics, and chemistry. Microscopic identification results concluded that willow and Chinese fir were the main wood species used to make this ship. The content of holocellulose in the ancient wood was only 37.9 to 38.9%, while the content of lignin was 55.2 to 56.4%. The cellulose crystallinity of ancient wood was 39 to 42% lower than that of healthy recent wood. Fourier transform infrared (FTIR) spectra revealed that the deterioration of ancient wood caused cellulose and hemicellulose degradation, but no apparent lignin alteration. The results could provide a basis for drawing up a conservation plan for the Nantong Ancient Ship. They could also provide a reference for the research and conservation of other archaeological shipwrecks in China.

DOI: 10.15376/biores.18.3.5028-5040

Keywords: Ancient wood; Deterioration; FTIR; Identification; XRD

*Contact information: a: School of Social Development, Nanjing Normal University, No. 1 Wenyuan Road, Qixia District, Nanjing, China; b: College of Furnishing and Industrial Design, Nanjing Forestry University, Str. Longpan No. 159, Nanjing, China; *Corresponding author: 13195@njnu.edu.cn*

RESEARCH AIMS

With the continuous improvement of archaeological science and technology, an increasing amount of wooden cultural relics are being discovered and excavated. In China, for the past 20 years, more than one ancient sunken ship has been excavated in the ocean or inland rivers, such as Huaguangjiao I (Shen *et al*. 2018; Liu *et al.* 2022b; Liu *et al.* 2023d), Nanhai I (Li *et al*. 2022), Xiaobaijiao I (Han *et al.* 2020), Luoyang I (Liu *et al.* 2023a), Taicang (Liu *et al.* 2023b), *etc.* These ancient shipwrecks had been buried in underground or underwater environments for hundreds of years and attacked by microorganisms, so they are very fragile (Donato *et al.* 2010; Jakes *et al.* 2015; Kilic and Kiliç 2018). To design suitable conservation processes, it is important to know the conservation status of ancient wood, including such parameters as wood species, density, chemical composition, *etc.*

In October 2022, an ancient shipwreck was excavated at an archaeological site in the Chongchuan district of Nantong city, China. Based on the ancient coins (Wanli period, 1572 to 1620) unearthed at the archaeological site, it was inferred that the ship belonged to the late Ming Dynasty. The ship is 9.9 m long, 3.1 m wide at the widest point, and 1.1 m deep. It comprises the following parts: bottom plate, bilge plate, body plate, deck, bulkhead plate, main keel, *etc.* Samples of wood extracted from the Nantong Ancient Ship were studied from the viewpoints of anatomy, physics, and chemistry. This paper

comprehensively analyzes the results and evaluates the wood samples. They could provide a basis for the drawing of a conservation plan for the Nantong Ancient Ship. They could also provide a reference for the research and conservation of other archaeological shipwrecks in China.

INTRODUCTION

In April 2022, a large number of stones were discovered at a construction site (E 118.80° and N 32.06°) in the Chongchuan district (Fig. 1), Nantong city, Jiangsu province, which was later identified as a Ming Dynasty hydraulic site after investigation by the cultural relics department. Excavations were carried out at the archaeological site from October 13, 2022 to December 18, 2022. Ancient ships were found in the northern part of the site. Many porcelain pieces, metal parts, tiles, and coins were found and are presumed to be from the late Ming Dynasty. The site proves that the course of a tributary of the Yangtze River passed through the place at the time.

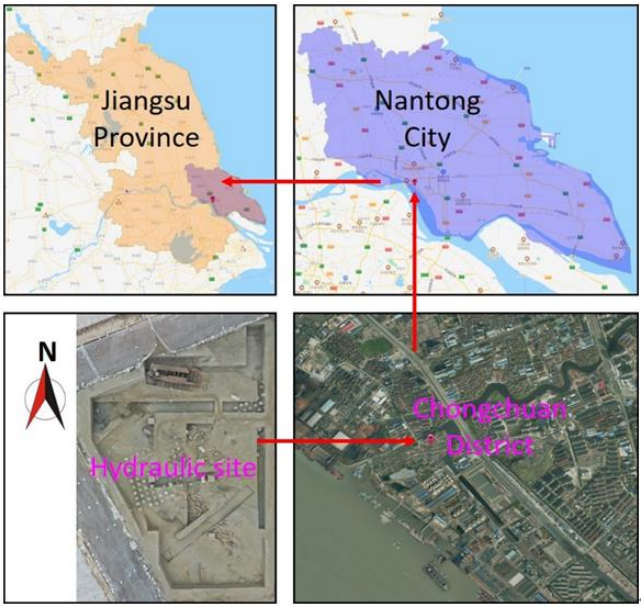

Fig. 1. Location of the Nantong hydraulic site

Generally, the decay of archaeological wood can be characterized by anatomical, physical, and chemical methods. Some basic parameters, such as basic density, water content, and residual basic density, are used to describe wood degradation (Gao *et al.* 2014; Macchioni *et al.* 2018; Endo and Sugiyama 2022). In addition, the degree of degeneration can be specified using different anatomical characteristics. The content of ash, α-cellulose, and total cellulose are usually used for the determination of wood health wood (Xia *et al.* 2018). They can also be used for the identification of waterlogged wood. Long-term degradation not only changes the content of cellulose in wood, but it also changes the existing state of cellulose (Łucejko *et al.* 2018; Broda and Popescu 2019). X-Ray diffraction (XRD) can be used to test the crystallinity of cellulose in ancient wood (Lionetto *et al.* 2014; Zhao *et al.* 2019; Sun *et al.* 2022). Environmental scanning electron microscopy (ESEM) is often used to collect the microscopic morphology of ancient wood

(Cha *et al.* 2014; Romagnoli *et al.* 2018; Stagno *et al.* 2021). Fourier transform infrared (FTIR) is a speedy way to monitor the chemical composition of wood and can indicate the chemical composition of ancient wood or naturally aged wood by changes in certain peaks (Pizzo *et al.* 2015; Han *et al.* 2022; Liu *et al.* 2022a).

In this article, wood decay was evaluated from anatomical, physical, and chemical perspectives. The microscopic structure of wood was observed by optical microscope and the species of wood were identified. The maximum water content, basic density, and residual basic density were determined, and the composition of the samples were analyzed. The crystallinity of cellulose in ancient wood was measured by XRD. The chemical composition changes of fresh wood and old wood were compared by FTIR. The microscopic morphology of ancient wood was observed by SEM.

EXPERIMENTAL

Materials

The samples were extracted from the Nantong Ancient Ship in December 2022. Table 1 lists the names of the samples and their respective positions on the ship. The positions are also marked in Fig. 2.

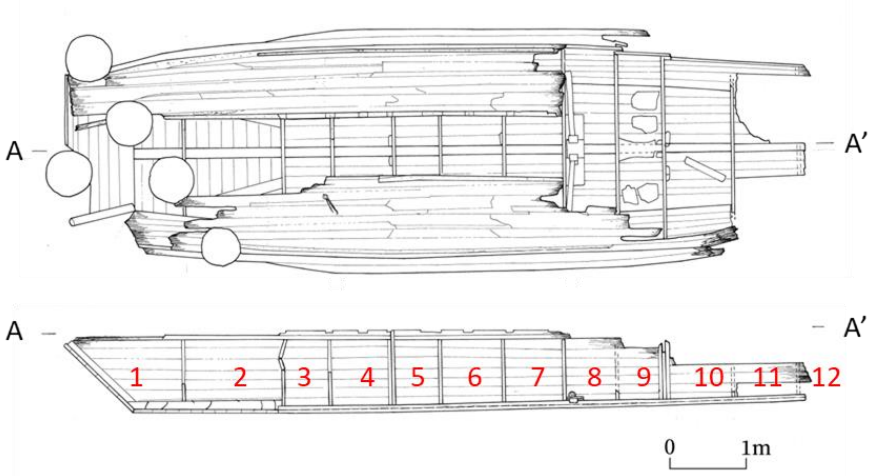

Fig. 2. Top view and section view of the Nantong Ancient Ship

Table 1. Sample Names and Sampling Positions

No.	Samples Names	Sampling Position
1	Bulkhead–1	Bulkheads of the 3rd and 4th cabins from the eastern part
2	Bulkhead–2	Bulkheads of the 4th and 5th cabins from the eastern part
3	Bulkhead–3	Bulkheads of the 5th and 6th cabins from the eastern part
4	Bulkhead–4	Bulkheads of the 6th and 7th cabins from the eastern part
5	Bilge strake–1	Bilge strake in the northern part
6	Bilge strake–2	Bilge strake in the southern part
7	Keel–1	Keel in the eastern part
8	Keel–2	Keel in the western part
9	Deck plating–1	Deck board in the northern part
10	Deck plating–2	Hull board in the southern part
11	Hull–1	Hull board in the northern part
12	Hull–2	Hull board in the southern part

Methods

Microscopic identification

Macro-characteristics are the basic information for wood identification. The cross-sections of specimens were observed with a 10× magnifying glass. The results showed that specimens 1 through 4 were diffuse-porous wood and 5 through 12 were coniferous wood. It was necessary to prepare microscopic slices and identify the species of wood by the microscopic structure of the specimens.

Because some of the wood samples were identified as soft and could not be sliced, the wood samples were first impregnated with 600 PEG (polyethylene glycol) for 3 days and then transferred to PEG 2000 for 3 days. The samples were then sliced by a microtome in transverse, radial, and tangential directions into slices of approximately 30 microns. All the slices were then stained with saffron and washed with distilled water, which increased the contrast of the microscopic images. The thin, stained, and transparent slices were observed at varying magnifications (40× to 100×) with an optical microscope (Zeiss Axio Scope A1 microscope, Carl Zeiss AG, Oberkochen, Germany) with AxioVision Rel.4.8 (Carl Zeiss AG, Oberkochen, Germany) under the mode of transmitted light. Finally, the species of wood were determined by comparing with relevant literature.

Determination of chemical composition

After being in the underwater/underground environment for a long time, the wood deteriorated to varying degrees, resulting in changes in its chemical composition. In this study, healthy recent wood of the same species was selected as a reference based on the identification results and changes in the chemical composition of the samples were compared. According to standard GB/T 2677.6-94 (1994) solvent extraction of wood and acid-insoluble lignin were determined. The fibrous raw material determination of holocellulose was determined according to GB/T 2677.10-94 (1994).

X-Ray diffraction

The extracted specimens and the healthy recent wood from the same wood species were surface-cleaned, dried, ground into 80-mesh powder, and pressed into sample sheets at room temperature. The samples were *in-situ* XRD analysed using the X'Pert Pro Multi-purpose diffractometer (PANalytical, Almelo, Netherlands) and the Rigaku Smart Lab 9 kW XRD system (Shimazu Co., Kyoto, Japan). In addition, the 2θ range was 5 to 40° at a rate of 2°/min. The spectrum provided was the average of three measurements of healthy recent wood and antique ship wood. Using the Segal method, the crystallinity of cellulose was calculated as the ratio of the peak area of the crystalline region to the total peak area, using the following Eq. 1 (Segal *et al.* 1959; Wang *et al.* 2023a),

$$CR_x = \frac{I_{002} - I_{AM}}{I_{002}} \times 100\% \quad (1)$$

where CR_x (%) denotes the degree of crystallinity of cellulose, I_{002} denotes diffraction intensity of the (002) lattice plane in cellulose, and I_{AM} indicates diffraction intensity of amorphous region (2θ = 18°).

Chemical structure analysis

To illustrate the chemical changes after deterioration, the extracted specimens and the healthy recent wood were ground into 80-mesh powder and pressed with KBr for FTIR testing. The device, a Tensor 27, Bruker, Ettlingen, Germany, has a spectral resolution of

4 cm^{-1} in the 4,000 cm^{-1} and 400 cm^{-1} range through 32 scans. After aligning the optical equipment, the background spectrum was collected before measurement. Furthermore, the spectrum presented referred to the average of three measurements for each sample of wood.

Morphological characteristics

To investigate possible changes in the physical aspects of wood samples from the Nantong Ancient Ship, the surface shape of wood samples was observed using an environmental scanning electron microscope (Quanta 200, FEI Company, Eindhoven, Netherlands). To increase the conductivity, ring sputtering was conducted by SEM with target 2" ID × 3" OD × 0.1 mm Anatech (SC502–314; Quorum Technologies Ltd., Watford, UK). The voltage used for SEM analysis was 20.0 kV.

RESULTS AND DISCUSSION

Microscopic Identification

Wood identification was completed through observing its macroscopic characteristics and microscopic structure. Macroscopic observation revealed that samples 1 through 4 were hardwood with diffuse-porous wood, and 5 through 12 were softwood.

Through analysis of the microscopic structure, samples 1 through 4 were the same wood species, identified as willow (*Salix* spp.) (Sauter and Wellenkamp 1988; Čufar *et al.* 2019; Wagenführ and Wagenführ 2021), as shown in Fig. 3. The growth rings of these samples—presented as thin lines—were slightly obvious. The samples showed diffuse-porous wood with uniseriate rays, many porous, size varying from small to very small, with uniform distribution.

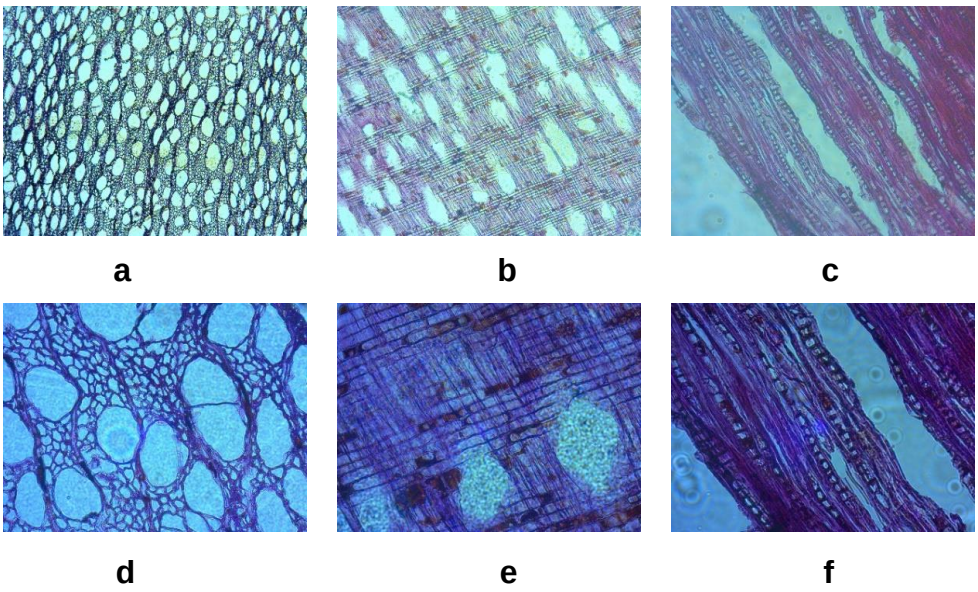

Fig. 3. Micrographs of investigated samples (1 through 4) magnifying 5× and 20× in transversal (a and d), tangential (b and e), and radial (c and f) sections

Most of the vessels were solitary pores—with a few vessels, usually 2 to 3, multiple pores—distributed in radial direction. The vessel perforations were single, with intervascular pitting interrow. The axial parenchyma was marginal parenchyma, very

small, 1 or 2 cells wide. In the radial section, heterogenous rays consisted of procumbent and upright cells. The uniseriate rays were 1 to 28 cells high, with most 5 to 20 cells high. The intercellular tract was not seen.

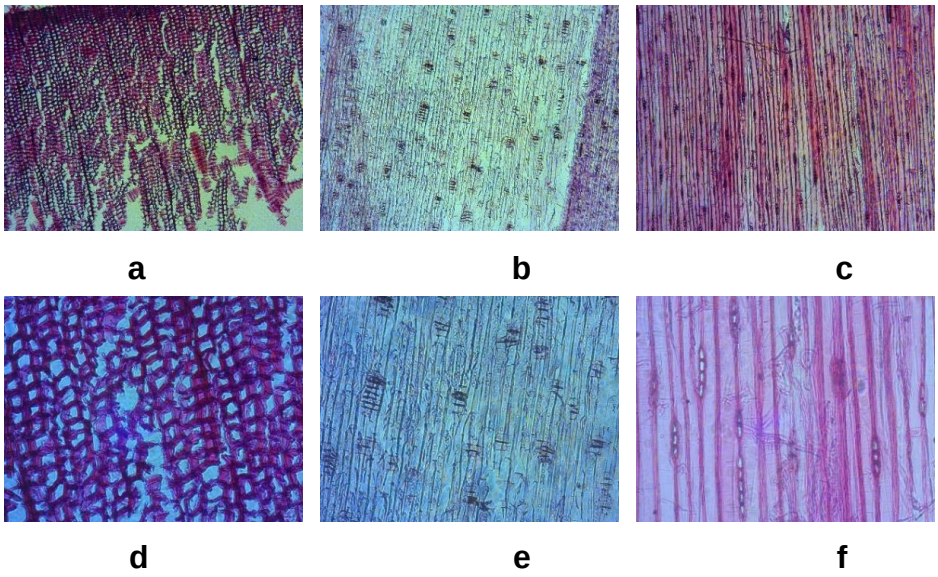

Fig. 4. Micrographs of investigated samples (5 through 12) magnifying 5× and 20× in transversal (a and d), tangential (b and e), and radial (c and f) sections

Microstructure observation of specimens 5 through 12 showed that they were the same wood species identified as Chinese fir (*Cunninghamia lanceolate*) (Caseldine *et al.* 2000; Sun *et al.* 2020; Tu *et al.* 2022). The growth rings of these wood specimens were obvious (Fig. 4). Between the growth rings, the color of late wood band was dark, and from early wood to late wood the color gradually lightened. The zone of the late wood was very narrow. Moreover, no resinous channels were observed. The tracheids did not show any helical thickenings. The bordered pit is usually listed on the radial wall of the tracheid. The amount of axial parenchyma was small, they appeared star-shaped and were scattered and distributed over both early wood and late wood. The uniseriate rays were 1 to 21 cells high, with most 5 to 13 cells high. The inner wall of the ray tracheid was not serrated. The cross-field pitting— type of pits characteristically from communication between rays and axial tracheids—was visible on the radial sections.

Willow and Chinese fir are common wood species in Nantong area. The results of wood identification revealed that people in the late Ming Dynasty were good at choosing local materials for making boats and ships. Many ancient ships made of Chinese fir wood—one of the most common woods used for shipmaking — have been excavated in China (Li *et al*. 2022; Liu *et al*. 2023d).

Determination of the Main Component Content

Long-term deterioration of the ancient wood modified its chemical composition, resulting in changes in its extraction content. Thus, extraction content is an important standard that reflects the degree of wood deterioration (Colombini *et al.* 2009; Liu *et al.* 2023c). According to the wood identification results, specimens 1 through 4 were willow, and specimens 5 through 12 were Chinese fir. They were divided into ancient willow (AW), ancient Chinese fir (ACF), healthy recent willow (HRW), and healthy recent

Chinese fir (HRCF) for comparison. The results in Table 2 show that the contents of alcohol-benzene and 1% NaOH extracts of the ancient wood—6.16% (AW), 7.08% (ACF), 12.75% (AW), and 14.26% (ACF)—were higher than the respective values of the healthy recent woods HRW and HRCF. In contrast, only 37.9% to 38.9% of holocellulose was found in the ancient wood, while healthy recent wood had 76.3% to 78.4% of holocellulose. This showed that cellulose and hemicellulose were seriously degraded into small molecules soluble in alcohol-benzene and NaOH and both were increased in extractives content (Table 2). Similarly, the content of acid-insoluble lignin in the ancient wood was much higher, reaching a maximum of 55.2% to 56.4% compared to 30.6% to 32.7% in healthy recent wood. This indicated that the total weight of wood decreased, and the lignin content increased after the degradation of holocellulose (Saxena and Gupta 2018).

Table 2. Chemical Compositions of Nantong Ancient Ship Wood and Healthy Recent Wood: Degradation

Wood Samples	Alcohol-benzene Extract (%)	1% NaOH Extract (%)	Acid Accumulator Insoluble Lignin (%)	Holocellulose (%)
AW	6.16(1.23) *	12.75(1.37) *	56.42 (1.29) *	37.86 (1.44) *
HRW	2.08(0.29) *	5.77(1.03) *	30.64 (1.86) *	78.43 (1.78) *
ACF	7.08(1.47) *	14.26(1.14) *	55.25 (2.11) *	38.94 (2.78) *
HRCF	1.97(0.43) *	6.35 (0.98) *	32.66(1.43) *	76.34 (2.16) *

* The data is presented as the average values (standard deviations in brackets)

X-Ray Diffraction

The presence of cellulose in wood is divided into crystalline and non-crystalline regions. The percentage of crystalline cellulose microfibril as a whole is called the crystallinity of cellulose, which is used to characterize the strength and deterioration of wood (Tamburini *et al.* 2017; Wang *et al.* 2023b). XRD is a common method used to determine the crystallinity of wood cellulose, which is usually determined by three peaks of 2θ at 18°, 22.5°, and 35°, respectively, as shown in Table 3. The crystallinity of AW and ACF were 23.6% and 25.8%, respectively, while that of HRW and HRCF were 40.6% and 41.7%, respectively. The results showed that the crystallinity of cellulose decreased by 39 to 42% in the long-time underwater/underground environment in Nantong. Studies have shown that bacterial and fungal invasion in underground environments degrades cellulose and hemicellulose, leading to a decrease in cellulose crystallinity.

Table 3. Chemical Compositions of Nantong Ancient Ship Wood and Healthy Recent Wood: Crystallinity

Wood Samples	2θ Peak Value (counts)		Crystallinity Degree of Cellulose (%)
	AM	002	
AW	4410(324) *	5769(425) *	23.56
HRW	6383(411) *	10743(426) *	40.58
ACF	4355(298) *	5868(365) *	25.78
HRCF	6252(321) *	10718(417) *	41.67

* The data are presented as the average values (standard deviations in brackets).

Chemical Structure Analysis Using FTIR Spectroscopy

Figure 5 shows the FTIR spectra of Nantong Ancient Ship wood and healthy recent wood. All spectra showed strong bands at 3320 cm^{-1}, consistent with the stretching

vibration of hydroxyl (-OH), C-H asymmetry, and symmetric stretching at 2850 to 2920 cm^{-1}. These peaks were slightly reduced in ancient wood, probably due to degradation of cellulose and hemicellulose (Andriulo *et al.* 2022; Longo *et al.* 2022). However, the peaks at 1371 cm^{-1} (CH deformation (symmetry)) and 1730 cm^{-1} (xylan C=O stretching vibration) in ancient wood carbohydrate only showed small peaks, almost none, belonging to the stretching vibration of xylan acetyl group ($CH_3C=O$) carbon-oxygen double bond (Bjurhager *et al.* 2012; Tamburini *et al.* 2014; Capano *et al.* 2015; Liu *et al.* 2023e). The concentrations of hemicellulose and cellulose were lower in the ancient wood samples. In contrast, the C=C stretching peak conforming to the aromatic ring (lignin) increased slightly at 1595 cm^{-1}. The peak value at 1508 cm^{-1} did not change significantly, indicating that the lignin concentration in ancient wood could be relatively increased, that is, only slight degradation occurred in the process of lignin degradation, which was consistent with previous studies (Popescu *et al.* 2006; Guo *et al.* 2020). In ancient wood, the deformation and vibration corresponding to primary alcohol C-O at 1022 cm^{-1} was significantly weakened, and the characteristics of β-chain corresponding to cellulose at 893 cm^{-1} almost disappeared. These changes further indicated the serious degradation of cellulose and hemicellulose (Gelbrich *et al.* 2012).

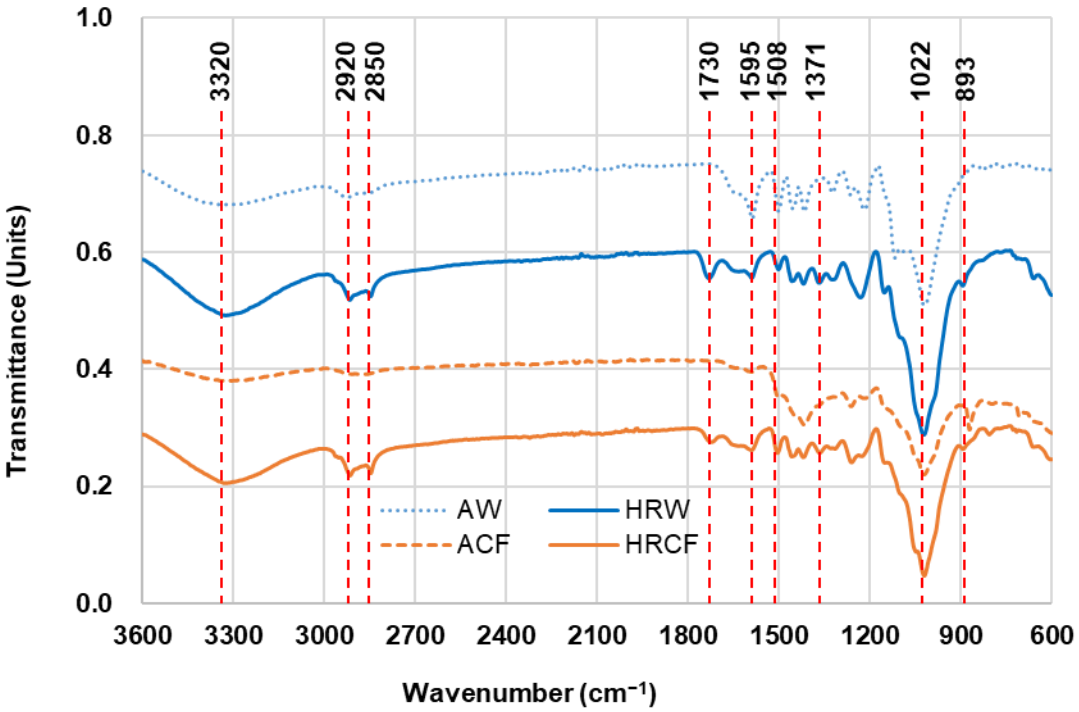

Fig. 5. FTIR spectra of Nantong Ancient Ship wood and healthy recent wood

Morphology

Degradation of cellulose and hemicellulose in wood may lead to changes in wood micromorphology. Potential changes in the physical structure of ancient wood caused by deterioration can be evaluated by the SEM images of its three sections, as shown in Fig. 6. On the cross-section, the duct cell wall was deformed obviously, because the strength of the degraded wood cell wall was reduced and the tension of water evaporation during the drying process was greater than the strength of the cell wall. Fragmentary material was found on the radial and tangential sections, also caused by the degradation of holocellulose.

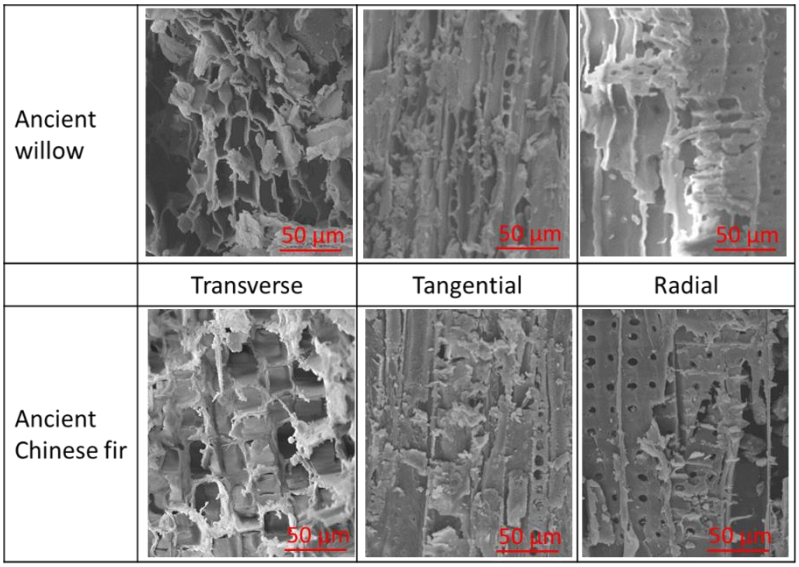

Fig. 6. SEM micrographs of old and new wood samples at 1400× magnification

CONCLUSIONS

1. Willow (*Salix* spp.) and Chinese fir (*Cunninghamia lanceolate*) were the main wood species used to make the Nantong Ancient Ship. These were important wood species for the ships and boats manufacturing at that time in the Nantong area.
2. The long-term underground deterioration led to the loss of cellulose and hemicellulose in the wood and the decrease of its mass, while the small change in the quality of lignin led to the increase of its relative content.
3. The degradation of cellulose also resulted in a 39 to 42% decrease in the crystallinity of cellulose.
4. The Fourier transform infrared (FTIR) spectra and scanning electron microscope (SEM) microscopic images further demonstrated that the degradation of cellulose and hemicellulose led to wood deterioration.

ACKNOWLEDGMENTS

This work was supported by the Nanjing Normal University Foundation for Basic Research (Grant No. 1309004).

REFERENCES CITED

Andriulo, F., Vespignani, L., Steindal, C. C., Bortolini, M., and de Ferri, L. (2022). "Evaluation of sol-gel hybrid nanocomposites for dry medieval wood," *Journal of Cultural Heritage* 56, 96-107. DOI: 10.1016/j.culher.2022.06.004

Bjurhager, I., Halonen, H., Lindfors, E. L., Iversen, T., Almkvist, G., Gamstedt, E. K., and Berglund, L. A. (2012). "State of degradation in archeological oak from the 17th century Vasa ship: Substantial strength loss correlates with reduction in (holo) cellulose molecular weight," *Biomacromolecules* 13(8), 2521-2527. DOI: 10.1021/bm3007456

Broda, M., and Popescu, C. M. (2019). "Natural decay of archaeological oak wood *versus* artificial degradation processes—An FT-IR spectroscopy and X-ray diffraction study," *Spectrochimica Acta Part A: Molecular and Biomolecular Spectroscopy* 209, 280-287. DOI: 10.1016/j.saa.2018.10.057

Capano, M., Pignatelli, O., Capretti, C., Lazzeri, S., Pizzo, B., Marzaioli, F., Martinelli, N., Gennarelli, I., Gigli, S., Terrasi, F., *et al*. (2015). "Anatomical and chemical analyses on wooden artifacts from a Samnite sanctuary in Hirpinia (Southern Italy)," *Journal of Archaeological Science* 57, 370-379. DOI: 10.1016/j.jas.2015.03.002

Caseldine, C. J., Baker, A., Charman, D. J., and Hendon, D. (2000). "A comparative study of optical properties of NaOH peat extracts: Implications for humi® cation studies," *The Holocene* 10(5), 649-658. DOI: 10.1191/095968300672976760

Cha, M. Y., Lee, K. H., and Kim, Y. S. (2014). "Micromorphological and chemical aspects of archaeological bamboos under long-term waterlogged condition," *International Biodeterioration & Biodegradation* 86(Part B), 115-121. DOI: 10.1016/j.ibiod.2013.08.008

Colombini, M. P., Lucejko, J. J., Modugno, F., Orlandi, M., Tolppa, E. L., and Zoia, L. (2009). "A multi-analytical study of degradation of lignin in archaeological waterlogged wood," *Talanta* 80(1), 61-70. DOI: 10.1016/j.talanta.2009.06.024

Čufar, K., Balzano, A., Krže, L., and Merela, M. (2019). "Wood identification using non-destructive confocal laser scanning microscopy," *Les/Wood* 68(2), 19-29. DOI: 10.26614/les-wood.2019.v68n02a02

Donato, D. I., Lazzara, G., and Milioto, S. (2010). "Thermogravimetric analysis A tool to evaluate the ability of mixtures in consolidating waterlogged archaeological woods," *Journal of Thermal Analysis and Calorimetry* 101, 1085-1091. DOI: 10.1007/s10973-010-0717-9

Endo, R., and Sugiyama, J. (2022). "New attempts with the keratin-metal/magnesium process for the conservation of archaeological waterlogged wood," *Journal of Cultural Heritage* 54, 53-58. DOI: 10.1016/j.culher.2022.01.002

Gao, J., Li, J., Qiu, J., and Guo, M. (2014). "Degradation assessment of waterlogged wood at Haimenkou site," *Frattura ed Integrità Strutturale* 8(30), 495-501. DOI: 10.3221/IGF-ESIS.30.60

GB/T 2677.6 (1994). "Fibrous raw material. Determination of solvent extractives," Standardization Administration of China, Beijing, China.

GB/T 2677.10 (1994). "Fibrous raw material. Fibrous raw material determination of holocellulose," Standardization Administration of China, Beijing, China.

Gelbrich, J., Mai, C., and Militz, H. (2012). "Evaluation of bacterial wood degradation by Fourier transform infrared (FTIR) measurements," *Journal of Cultural Heritage* 13(3, Supplement), S135-S138. DOI: 10.1016/j.culher.2012.03.003

Guo, J., Zhang, M., Liu, J., Luo, R., Yan, T., Yang, T., Jiang, X., Dong, M., and Yin, Y. (2020). "Evaluation of the deterioration state of archaeological wooden artifacts: A nondestructive protocol based on direct analysis in real time - mass spectrometry (DART-MS) coupled to chemometrics," *Analytical Chemistry* 92(14), 9908-9915. DOI: 10.1021/acs.analchem.0c01429

Han, L., Guo, J., Tian, X., Jiang, X., and Yin, Y. (2022). "Evaluation of PEG and sugars consolidated fragile waterlogged archaeological wood using nanoindentation and ATR-FTIR imaging," *International Biodeterioration & Biodegradation* 170, article ID 105390. DOI: 10.1016/j.ibiod.2022.105390

Han, L., Guo, J., Wang, K., Gronquist, P., Li, R., Tian, X., and Yin, Y. (2020). "Hygroscopicity of waterlogged archaeological wood from Xiaobaijiao No.1 shipwreck related to its deterioration state," *Polymers* 12(4), article 834. DOI: 10.3390/polym12040834

Jakes, J. E., Hunt, C. G., Yelle, D. J., Lorenz, L., Hirth, K., Gleber, S. C., Vogt, S., Grigsby, W., and Frihart, C. R. (2015). "Synchrotron-based X-ray fluorescence microscopy in conjunction with nanoindentation to study molecular-scale interactions of phenol-formaldehyde in wood cell walls," *ACS Applied Materials & Interfaces* 7(12), 6584-6589. DOI: 10.1021/am5087598

Kilic, N., and Kiliç, A. G. (2018). "Analysis of waterlogged woods: Example of Yenikapi Shipwreck," *Art-Sanat Dergisi* 9, 1-11.

Li, R., Guo, J., Macchioni, N., Pizzo, B., Xi, G., Tian, X., Chen, J., Jiang, X., Cao, J., Zhang Q., *et al.* (2022). "Characterisation of waterlogged archaeological wood from Nanhai No. 1 shipwreck by multidisciplinary diagnostic methods," *Journal of Cultural Heritage* 56, 25-35. DOI: 10.1016/j.culher.2022.05.004

Lionetto, F., Quarta, G., Cataldi, A., Cossa, A., Auriemma, R., Calcagnile, L., and Frigione, M. (2014). "Characterization and dating of waterlogged woods from an ancient harbor in Italy," *Journal of Cultural Heritage* 15(2), 213-217. DOI: 10.1016/j.culher.2013.02.003

Liu, X., Ma, W., Tu, X., Huang, H., and Varodi, A. M. (2023a). "Study on the wood characteristics of the Chinese Ancient Ship Luoyang I," *Materials* 16(3), article 1145. DOI: 10.3390/ma16031145

Liu, X., Timar, M. C., Varodi, A. M., Nedelcu, R., and Torcătoru, M. J. (2022a). "Colour and surface chemistry changes of wood surfaces coated with two types of waxes after seven years exposure to natural light in indoor conditions," *Coatings* 12(11), article 1689. DOI: 10.3390/coatings12111689

Liu, X., Tu, X., Ma, W., Zhang, C., Huang, H., and Varodi, A. M. (2022b). "Consolidation and Dehydration of waterlogged archaeological wood from Site Huaguangjiao No. 1," *Forests* 13(11), article 1919. DOI: 10.3390/f13111919

Liu, X., Xu, X., Tu, X., Ma, W., Huang, H., and Varodi, A. M. (2023b). "Characteristics of ancient ship wood from Taicang of the Yuan Dynasty," *Materials* 16(1), article 104. DOI: 10.3390/ma16010104

Liu, X., Yang, S., Zhang, C., Huang, H., and Varodi, A. M. (2023c). "Comparative study on slow pyrolysis products of abandoned furniture materials," *BioResources* 18(1), 629-640. DOI: 10.15376/biores.18.1.629-640

Liu, X., Zhu, L., Tu, X., Zhang, C., Huang, H., and Varodi, A. M. (2023d). "Characteristics of ancient shipwreck wood from Huaguang Jiao No. 1 after desalination," *Materials* 16(2), article 510. DOI: 10.3390/ma16020510

Liu, X., Zhang, C., Yang, S., and Varodi, A. (2023e). "Effects of pyrolysis process on products yield of plywood from abandoned furniture," *Wood Research* 68(2), 348-359. DOI: 10.37763/wr.1336-4561/68.2.348359

Longo, S., Corsaro, C., Granata, F., and Fazio, E. (2022). "Clinical CT densitometry for wooden cultural heritage analysis validated by FTIR and Raman spectroscopies,"

Radiation Physics and Chemistry 199, article ID 110376. DOI: 10.1016/j.radphyschem.2022.110376

Łucejko, J. J., Mattonai, M., Zborowska, M., Tamburini, D., Cofta, G., Cantisani, E., Kúdela, J., Cartwright, C., Colombini, M. P., Ribechini, E., and Modugno, F. (2018). "Deterioration effects of wet environments and brown rot fungus *Coniophora puteana* on pine wood in the archaeological site of Biskupin (Poland)," *Microchemical Journal* 138, 132-146. DOI: 10.1016/j.microc.2017.12.028

Macchioni, N., Pecoraro, E., and Pizzo, B. (2018). "The measurement of maximum water content (MWC) on waterlogged archaeological wood: A comparison between three different methodologies," *Journal of Cultural Heritage* 30, 51-56. DOI: 10.1016/j.culher.2017.10.005

Pizzo, B., Pecoraro, E., Alves, A., Macchioni, N., and Rodrigues, J. C. (2015). "Quantitative evaluation by attenuated total reflectance infrared (ATR-FTIR) spectroscopy of the chemical composition of decayed wood preserved in waterlogged conditions," *Talanta* 131, 14-20. DOI: 10.1016/j.talanta.2014.07.062

Popescu, C., Vasile, C., Popescu, M., Singurel, G., Popa, V. I., and Munteanu, B. S. (2006). "Analytical methods for lignin characterization. II. Spectroscopic studies," *Cellulose Chemistry and Technology* 40(8), 597-622.

Romagnoli, M., Galotta, G., Antonelli, F., Sidoti, G., Humar, M., Kržišnik, D., Čufar, K. and Petriaggi, B. D. (2018). "Micro-morphological, physical and thermogravimetric analyses of waterlogged archaeological wood from the prehistoric village of Gran Carro (Lake Bolsena-Italy)," *Journal of Cultural Heritage* 33, 30-38. DOI: 10.1016/j.culher.2018.03.012

Sauter, J. J., and Wellenkamp, S. (1988). "Protein storing vacuoles in ray cells of willow wood (*Salix caprea* L.)," *IAWA Journal* 9(1), 59-65.

Saxena, M., and Gupta, M. K. (2018). "Hybrid mango/*Shorea robusta* wood reinforced epoxy composite: Crystalline behavior and dynamic mechanical analysis," *Materials Today: Proceedings* 5(9), 19359-19366. DOI: 10.1016/j.matpr.2018.06.295

Segal, L., Creely, J. J., Martin, Jr., A. E., and Conrad, C. M. (1959). "An empirical method for estimating the degree of crystallinity of native cellulose using the X-ray diffractometer," *Textile Research Journal* 29(10), 786-794. DOI: 10.1177/004051755902901003

Shen, D., Li, N., Fu, Y., Macchioni, N., Sozzi, L., Tian, X., and Liu, J. (2018). "Study on wood preservation state of Chinese ancient shipwreck Huaguangjiao I," *J. Cult. Herit.* 32, 53-59. DOI: 10.1016/j.culher.2018.01.009

Stagno, V., Egizi, F., Corticelli, F., Morandi, V., Valle, F., Costantini, G., Longo, S., and Capuani, S. (2021). "Microstructural features assessment of different waterlogged wood species by NMR diffusion validated with complementary techniques," *Magnetic Resonance Imaging* 83, 139-151. DOI: 10.1016/j.mri.2021.08.010

Sun, G. R., He, Y. R., and Wu, Z. H. (2022). "Effects of thermal treatment on the dimensional stability and chemical constituents of new and aged camphorwood," *BioResources* 17(3), 4186-4195. DOI: 10.15376/biores.17.3.4186-4195

Sun, H., Jia, R., Wu, Y-H., Zhou, L., Liu, S. Q., and Wang, Y. R. (2020). "Rapid detection of microstructural characteristics of heartwood and sapwood of Chinese fir clones," *Spectroscopy and Spectral Analysis* 40(1), 184-188.

Tamburini, D., Łucejko, J. J., Modugno, F., Colombini, M. P., Pallecchi, P., and Giachi, G. (2014). "Microscopic techniques (LM, SEM) and a multi-analytical approach (EDX, FTIR, GC/MS, Py-GC/MS) to characterise the decoration technique of the

wooden ceiling of the House of the Telephus Relief in Herculaneum (Italy)," *Microchemical Journal* 116, 7-14. DOI: 10.1016/j.microc.2014.03.008

Tamburini, D., Łucejko, J. J., Pizzo, B., Mohammed, M. Y., Sloggett, R., and Colombini, M. P. (2017). "A critical evaluation of the degradation state of dry archaeological wood from Egypt by SEM, ATR-FTIR, wet chemical analysis and Py (HMDS)-GC-MS," *Polymer Degradation and Stability* 146, 140-154. DOI: 10.1016/j.polymdegradstab.2017.10.009

Tu, X. W., Liu, X. Y., and Varodi, A. M. (2022). "Characterization and identification of wooden rice bucket made in 1860s," *BioResources* 17(4), 6511-6520. DOI: 10.15376/biores.17.4.6511-6520

Wagenführ, R., and Wagenführ, A. (2021). *Holzatlas, Hanser Fachbuchverlag [Transwood, Trahanse Press], Carl Hanser Verlag GmbH Co KG*, Munich, Germany.

Wang, B., Nie, Y., Kang, Z., and Liu, X. (2023a). "Effects of coagulating conditions on the crystallinity, orientation and mechanical properties of regenerated cellulose fibers," *International Journal of Biological Macromolecules* 225, 1374-1383. DOI: 10.1016/j.ijbiomac.2022.11.195

Wang, J., Han, X., Wu, W., Wang, X., Ding, L., Wang, Y., Li, S., Hu, J., Yang, W., Zhang, C., *et al.* (2023b). "Oxidation of cellulose molecules toward delignified oxidated hot-pressed wood with improved mechanical properties," *International Journal of Biological Macromolecules* 231, article ID 123343. DOI: 10.1016/j.ijbiomac.2023.123343

Xia, Y., Chen, T. Y., Wen, J. L., Zhao, Y. L., Qiu, J., and Sun, R. C. (2018). "Multi-analysis of chemical transformations of lignin macro-molecules from waterlogged archaeological wood," *International Journal of Biological Macromolecules* 109, 407-416. DOI: 10.1016/j.ijbiomac.2017.12.114

Zhao, C., Zhang, X., Liu, L., Yu, Y., Zheng, W., and Song, P. (2019). "Probing chemical changes in holocellulose and lignin of timbers in ancient buildings," *Polymers* 11(5), article 809. DOI: 10.3390/polym11050809

Article submitted: March 24, 2023; Peer review completed: April 29, 2023; Revised version received and accepted: May 11, 2023; Published: June 1, 2023.
DOI: 10.15376/biores.18.3.5028-5040